



Azo-containing pyridine amide ligand. A six-coordinate nickel(II) complex and its one-electron oxidized species: Structure and properties

Anuj Kumar Sharma, Saikat Biswas, Suman Kumar Barman, Rabindranath Mukherjee*

Department of Chemistry, Indian Institute of Technology Kanpur, Kanpur 208 016, India

ARTICLE INFO

Article history:

Received 17 February 2010
Received in revised form 18 March 2010
Accepted 23 March 2010
Available online 27 March 2010

Dedicated to Professor Animesh Chakravorty on the occasion of his 75th birthday

Keywords:

Azo group containing pyridine amide ligand
Ni(II) complex
Crystal structure
Redox properties
Electrochemically-generated nickel(III)
EPR spectra

ABSTRACT

A new potentially tridentate ligand HL¹¹ consisting of 2-pyridinecarboxamide unit and azo functionality has been used, in its deprotonated form, to prepare a nickel(II) complex which has been structurally characterized. The ligand L¹¹(–) affords a bis-complex [Ni^{II}(L¹¹)₂] (1). In 1, the two L¹¹(–) ligands bind to the Ni^{II} center in a *mer* configuration. The relative orientations within the pairs of pyridyl-N, deprotonated amido-N, and azo-N atoms are *cis*, *trans*, and *cis*, respectively. The Ni^{II}N₂(pyridyl)N₂(amide)N₂(azo) coordination environment is severely distorted from ideal octahedral geometry. The Ni–N_{am} (am = amide) bond lengths are the shortest and the Ni–N_{azo} bond lengths are the longest. Complex 1 exhibits a quasi-reversible Ni^{III}/Ni^{II} redox process. Moreover, the complex displays two ligand-centered (azo group) quasi-reversible redox processes. Spectroscopic (absorption and EPR) properties have been studied on coulometrically-generated nickel(III) species. To understand the nature of metal–ligand bonding interactions Density Functional Theory (DFT) calculations have been performed on 1 at the B3LYP level of theory. Calculations have also been done for closely related nickel(II) complexes of deprotonated pyridine amide ligands and comparative discussion has been made using observed results.

© 2010 Elsevier B.V. All rights reserved.

1. Introduction

Amide bonds are ubiquitous in biochemistry, because they provide the linkages that held together two of the most important types of biopolymers, nucleic acids and proteins. The interest in the study of amide complexes [1] derives from their ability to model active sites present in some metallo-proteins [2], to act as effective catalysts for important organic transformations [1,3], and the search for a better understanding of the physicochemical properties of such complexes, especially to modulate the structural, stereochemical, and electronic properties of transition metal centers [1,4–10]. From this perspective, the ligand systems based upon 2-pyridinecarboxamide [1,4–7] and 2,6-pyridinecarboxamide [1,8–10] are noteworthy. Using electronically/sterically demanding pyridine/pyrazine amide ligands HL¹–H₂L¹⁰ (Fig. 1), in their deprotonated form, we have developed interesting coordination chemistry of a variety of transition metal ions to demonstrate noteworthy molecular structural, electronic structural, and redox properties [4,8].

In pursuit of designing new pyridine amide ligands that will incorporate azo functionality (well known group as π -acceptors

* Corresponding author. Tel.: +91 512 2597437; fax: +91 512 2597436.
E-mail address: rnm@iitk.ac.in (R. Mukherjee).

[11,12] to stabilize low oxidation state of metal ions) in this work we have directed our attention to a new ligand HL¹¹. In order to evaluate the ability of this new potentially tridentate 2-pyridinecarboxamide ligand, appended with azo functionality, to modulate the structural and electronic properties of transition metal ions, we have chosen nickel(II) as a test case. To reveal the stereochemical changes around the nickel(II) center caused by ligand-structure modification of deprotonated pyridine/pyrazine amide ligands upon changing from L⁴(2–) [8c]/L⁵(2–) [6o]/L⁹(2–) [6n]/L^{9'}(2–) [4d] to L¹¹(–) (Fig. 1), we have determined the crystal structure of the new complex [Ni^{II}(L¹¹)₂] (1), revealing Ni^{II}(N_{pyridine})₂–(N_{amide})₂(N_{azo})₂ coordination environment. Room-temperature magnetic and spectroscopic properties of 1 have also been investigated. Given the strong σ -donating properties of amide ligands [1,13] and encouraged by our previous experience [4c,8c] of generating/isolating nickel(III) and nickel(IV) complexes [14] we wished to investigate whether or not for the present complex such a possibility exists. Cyclic voltammetric experiments reveal that stabilization of nickel(III) state could be achieved with new deprotonated ligand L¹¹(–). We report the characterization of coulometrically-generated one-electron oxidized form of 1 and confirm that the oxidation process is metal-centered (EPR spectra). Moreover, as it has been demonstrated that pyridine amide ligands

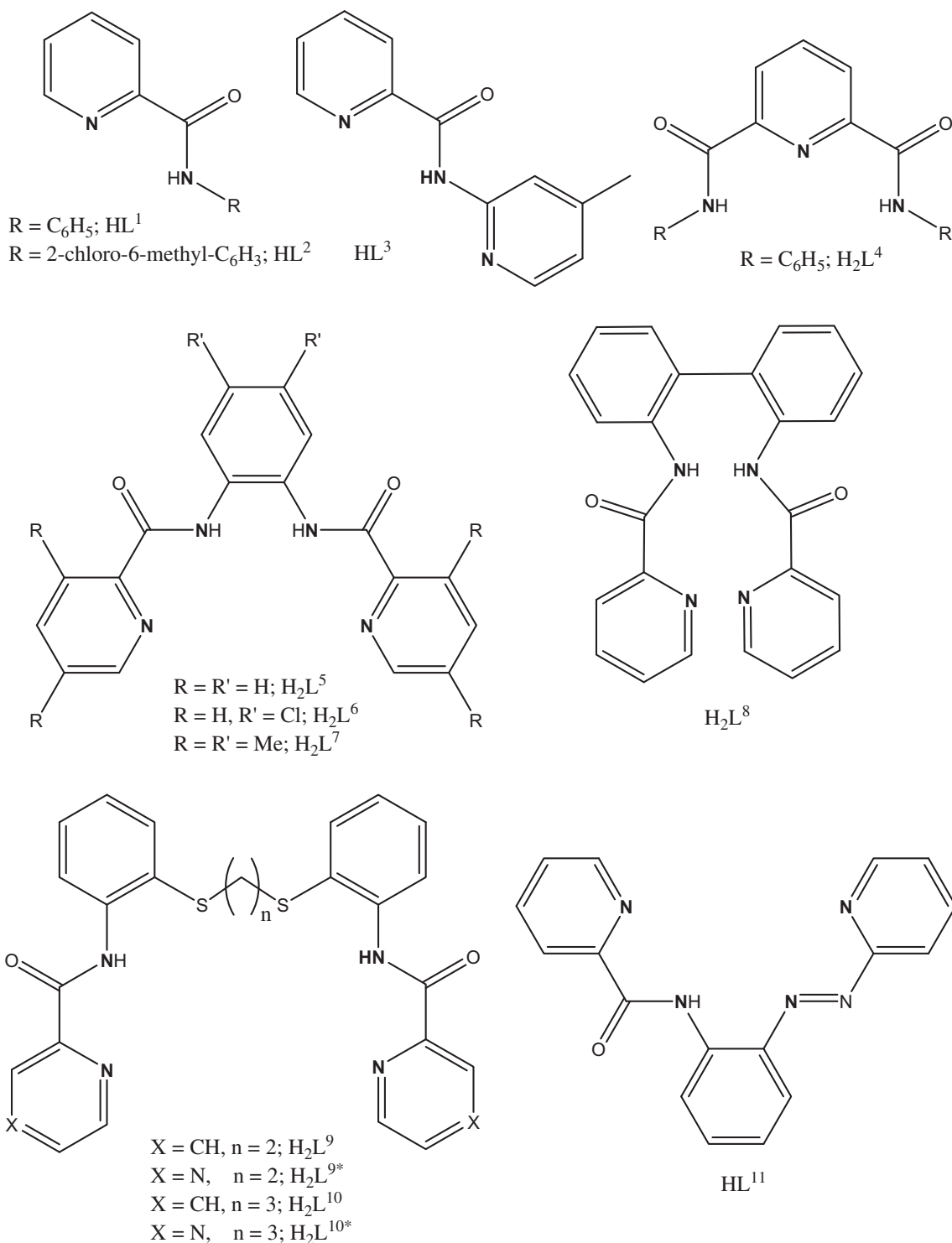


Fig. 1. The ligands of our concern.

are non-innocent [4e,6b,7,8a,15] we have investigated the nature of metal–ligand bonding interactions in **1** and two reported six-coordinate nickel(II) complexes with $Ni^{II}(N_{\text{pyridine}})_2(N_{\text{amide}})_4$ [**8c**] and $Ni^{II}(N_{\text{pyridine}})_2(N_{\text{amide}})_2(S_{\text{thioether}})_2$ [**4d**] coordination sphere. This analysis has given us an opportunity to rationalize the trend in $E_{1/2}$ values of the Ni^{III}/Ni^{II} redox process for the chosen group of complexes.

2. Experimental

2.1. Materials

All reagents were obtained from commercial sources and used as received. Solvents were dried and purified according to reported procedures [4,8]. Tetra-*n*-butylammonium perchlorate (TBAP) was

prepared and purified as before. 2-(phenylazo)aniline was synthesized following a reported methodology [16].

2.2. Synthesis of the ligand and the complex

2.2.1. Synthesis of 2-[N-(2-phenylazo)carbamoyl]pyridine

A solution of 2-(phenylazo)aniline (1.5 g, 7.6 mmol) in dry THF (50 mL) was taken in a 100 mL two-necked round bottom flask. To it pyridine-2-carbonylchloride (1.4 g, 7.85 mmol) and triethylamine (0.8 g 7.85 mmol) was added and the mixture was stirred for 24 h in N₂ atmosphere. It was then filtered and the residue was washed with chloroform. The filtrate was concentrated under reduced pressure. An oily compound thus obtained was subjected to column chromatography [ethyl acetate and *n*-hexane (2:98), as mobile phase] over silica gel (100–200 mesh). After solvent removal the purified compound was obtained as orange-yellow crystalline solid. Yield: 1.46 g (64%). IR (KBr, cm⁻¹): 3309 ν(N–H)_{str}, 1524 ν(N–H)_{bend}; 1685 ν(C=O)_{str}. ¹H NMR (in CDCl₃, 400 MHz): δ (in ppm) 8.91 (1H, d, py-H₁), 8.39 (1H, d, py-H₄), 8.34 (1H, d, py-H₃), 8.13 (2H, d, Ph-H₉ and H₁₃); 7.9411 (2H, t, Ph-H₅ and Ph-H₈); 7.506–7.605 (3H, m, Ph-H₁₀, Ph-H₁₁, Ph-H₁₂ and 1H, m, py-H₂); 7.211–7.288 (2H, q, Ph-H₇ and Ph-H₆).

2.2.2. Synthesis of [Ni^{II}(L¹¹)₂] (1)

The ligand (0.1 g, 0.34 mmol) was dissolved in MeOH (10 mL) and to it was added Ni^{II}(O₂CMe)₂·4H₂O (0.041 g, 0.17 mmol) in portions. The color of the solution changed from light-orange to dark brown. The mixture was stirred for 2 h. After removal of solvent a black solid was obtained, which was recrystallized from MeOH/Et₂O affording black shining crystals. Yield: 0.08 g (~73%). IR (KBr, cm⁻¹, selected peaks): 1620 ν(C=O str). Absorption spectrum [λ_{max}/nm (ε/M⁻¹ cm⁻¹)] (in CH₂Cl₂): 900 (10), 480 (10 200), 330 (21 700), 260 (24 100).

2.3. Measurements

Elemental analyses were obtained using a Thermo Quest EA 1110 CHNS-O, Italy. Spectroscopic measurements were made using the following instruments: IR (KBr, 4000–600 cm⁻¹), Bruker Vector 22; electronic, Agilent 8453 diode-array spectrophotometer. ¹H NMR spectra (CDCl₃ solution) were obtained on a JEOL JNM LA 400 (400 MHz) spectrophotometer. Chemical shifts are reported in ppm referenced to TMS and/or deuterated solvent peaks. X-band EPR spectral measurements were obtained using Bruker EMX 1444 spectrometer (fitted with a quartz Dewar for measurement at 120 K). The EPR spectra were calibrated with diphenylpicrylhydrazyl, DPPH (*g* = 2.0037). Spectra were treated by using the Bruker WINEPR software and simulated using the Bruker SIMFONIA software.

Cyclic voltammetric measurements were performed by using a CH Instruments Electrochemical Analyzer/Workstation Model 600B Series. A standard three-electrode cell was employed with a Beckman (M-39273) platinum-inlay working electrode, a platinum-wire auxiliary electrode, and a saturated calomel electrode (SCE) as reference; no correction was made for liquid junction potential. Potentials were recorded at 298 K. Uncompensated solution resistance in the cell configuration was minimized by placing the reference electrode tip as close to the working electrode as possible and using an approximately constant ratio of TBAP and solute concentration (~1.0 mM and 0.1 M, respectively). Coulometric oxidation was achieved at 298 K using a platinum mesh. Spectroelectrochemical measurements were performed using a custom-made cell (Model EF-1350) from Bioanalytical Systems Inc., USA.

Room-temperature magnetic susceptibility measurements were made on polycrystalline samples (powder form) of **1** by Faraday method using a locally-built magnetometer. The details of the

setup are described elsewhere [8d]. Effective magnetic moment was calculated from $\mu_{\text{eff}} = 2.828[\chi_{\text{M}}T]^{1/2}$, where χ_{M} is the corrected molar susceptibility. The diamagnetic corrections [17] were applied to the susceptibility data.

Density Functional Theory (DFT) calculations were performed with Becke's three-parameter hybrid exchange functional [18], and the Lee–Yang–Parr correlation functional (B3LYP) [19]. The atomic coordinates of all the complexes were taken from their X-ray structures. The 6-311G(d) basis set was used for the metal center. For H, C, N, and O atoms 6-31G-(d) basis set was used. All calculations were performed with the GAUSSIAN 03 (G03) suite of programs [20]. Orbital diagrams were generated at isosurface of 0.02 using GAUSSVIEW 3.0 [21].

2.4. Crystal structure determination

Single-crystal of suitable dimension was used for data collection. Diffraction intensities were collected on a Bruker SMART APEX CCD diffractometer, with graphite-monochromated Mo K α ($\lambda = 0.71073$ Å) radiation at 100(2) K. For data reduction 'Bruker Saint Plus' program was used. The data were corrected for Lorentz and polarization effects; empirical absorption correction (SADABS) was applied. Structure was solved by SIR-97 and refined by full-matrix least-squares methods based on F^2 using SHELXL-97, incorporated in wingX 1.64 crystallographic collective package [22]. The position of the hydrogen atoms were calculated by assuming ideal geometries, but not refined. For **1** all non-hydrogen atoms were refined anisotropically. Pertinent crystallographic parameters are summarized in Table 1.

3. Results and discussion

3.1. Synthesis and properties

Our general familiarity with pyridine/pyrazine amide ligands [4,8] has prompted us, for viable azo group coordination, to employ

Table 1
Data collection and structure refinement parameters for [Ni^{II}(L¹¹)₂] (1).

Compound	1
Chemical formula	C ₄₀ H ₃₆ NiN ₆ O ₄
Formula weight	751.48
Crystal color, habit	Brown, block
Crystal size (mm)	0.10 × 0.10 × 0.09
<i>T</i> (K)	100(2)
λ (Å)	0.71073
Crystal system	Monoclinic
Space group	<i>P</i> ₂ / <i>n</i> (#14)
<i>a</i> (Å)	12.563(2)
<i>b</i> (Å)	18.544(3)
<i>c</i> (Å)	15.212(3)
α (°)	90
β (°)	94.409(4)
γ (°)	90
<i>V</i> (Å ³)	3533.3(11)
<i>Z</i>	4
ρ_{calc} (g cm ⁻³)	1.413
μ (mm ⁻¹)	0.604
<i>F</i> (0 0 0)	1568
Total reflections	22 992
Unique reflections [<i>R</i> _{int}]	8636 [<i>R</i> _{int} = 0.0931]
Observed reflections [<i>I</i> > 2 σ (<i>I</i>)]	4743
Number of parameters	480
Final <i>R</i> indices [<i>I</i> > 2 σ (<i>I</i>)]	<i>R</i> ₁ = 0.0678 ^a <i>wR</i> ₂ = 0.1585 ^b
<i>R</i> indices (all data)	<i>R</i> ₁ = 0.1344 ^a <i>wR</i> ₂ = 0.2188 ^b
Goodness-of-fit on F^2	1.003

^a $R_1 = \sum(|F_o| - |F_c|)/\sum|F_o|$.

^b $wR_2 = \{\sum[w(|F_o|^2 - |F_c|^2)^2]/\sum[w(|F_o|^2)^2]\}^{1/2}$.

an interesting combination of both pyridine amide and azo functionality in a single ligand system. In pursuit of such a ligand we set out a reaction between 2-(phenylazo)aniline [16] and pyridine-2-carbonylchloride in 1:1 molar ratio in presence of triethylamine. The outcome of such an endeavor is the successful synthesis of 2-[N-(2-phenylazo)carbamoyl]pyridine (HL¹¹). The new ligand was characterized by its ¹H NMR spectrum [Fig. S1 (Supporting material)]. The ligand in its deprotonated form L¹¹(-) offers three very different kinds of N-donor atoms, viz., a pyridyl-N, a deprotonated amido-N, and an azo-N. Notably, pyridyl-N and azo-N are π -accepting and amido-N is strongly σ -donating.

Reaction of HL¹¹ with Ni(O₂CMe)₂·4H₂O in 2:1 molar ratio in MeOH after usual workup gave [Ni^{II}(L¹¹)₂] (1) as shining black crystalline compound. The N–H stretching frequency of the free ligand (3309 cm⁻¹) is absent in the IR spectrum of the nickel(II) complex, confirming that the ligand is coordinated in the deprotonated form. Coordination of the deprotonated carboxamido nitrogen to the nickel(II) center results in a red shift in the carbonyl stretching frequency from 1685 cm⁻¹ in the free ligand (HL¹¹) to 1620 cm⁻¹ in the complex.

The complex 1 is soluble in common organic solvents such as MeOH, CH₂Cl₂, CHCl₃, and MeCN to give deep brownish red solutions. The color arises from two strong ligand-to-metal charge-transfer (LMCT) band at 330 nm and 480 nm. A low intensity crystal field transition is observed at 900 nm, which is assigned as due to ³A_{2g} → ³T_{2g} transition (in octahedral parentage) [4d,8c]. Still higher energy transition at 260 nm is due to metal-perturbed intraligand charge-transfer. The absorption spectrum is displayed in Fig. 2.

The effective magnetic moment of 1 is 2.98 μ_B (300 K), corresponding to an S = 1 state, with an appreciable orbital contribution [4d,8c].

3.2. Description of the structure

A perspective view of the metal coordination environment in 1 is shown in Fig. 3. Table 2 contains selected bond length and bond angles. The nickel(II) ion is coordinated to two potentially tridentate L¹¹(-) ligands. Thus HL¹¹, in its deprotonated form, utilizes all its donor sites for metal coordination and the arrangement of two L¹¹(-) ligands are in meridional form. The Ni(II) center is coordinated by two pyridyl nitrogens [N(1) and N(5)], two deprotonated amide nitrogens [N(2) and N(6)], and two azo nitrogens [N(3) and N(7)]. The relative orientations within the pairs of pyri-

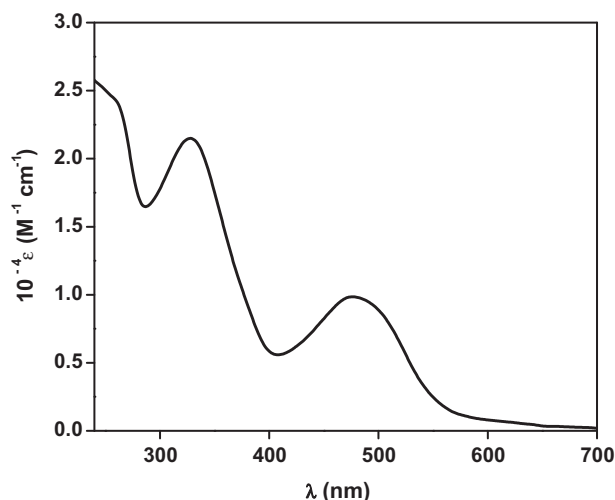


Fig. 2. Absorption spectrum (250–700 nm) of [Ni^{II}(L¹¹)₂] (1) in CH₂Cl₂.

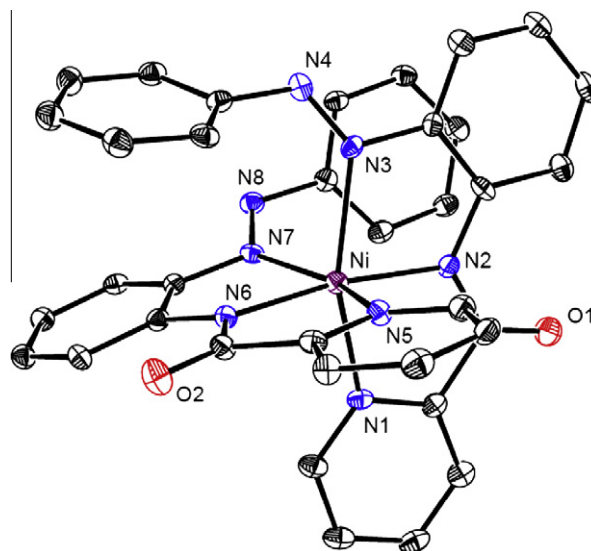


Fig. 3. Perspective view of [Ni^{II}(L¹¹)₂] (1). Carbon atoms are not labelled and hydrogen atoms are omitted for clarity.

Table 2
Selected bond lengths (Å) and angles (°) in 1.

Ni–N(1)	2.087(3)	N(1)–Ni–N(2)	80.01(14)
Ni–N(2)	1.994(3)	N(1)–Ni–N(3)	157.35(14)
Ni–N(3)	2.196(3)	N(1)–Ni–N(5)	93.65(13)
Ni–N(5)	2.087(3)	N(1)–Ni–N(6)	93.28(14)
Ni–N(6)	2.008(3)	N(1)–Ni–N(7)	94.05(13)
Ni–N(7)	2.189(3)	N(2)–Ni–N(3)	78.48(14)
N(3)–C(12)	1.417(5)	N(2)–Ni–N(5)	94.53(14)
N(4)–C(13)	1.412(5)	N(2)–Ni–N(6)	171.17(14)
N(5)–C(19)	1.335(5)	N(2)–Ni–N(7)	107.65(13)
N(5)–C(23)	1.352(5)	N(3)–Ni–N(5)	95.04(13)
N(6)–C(24)	1.340(5)	N(3)–Ni–N(6)	108.80(13)
N(6)–C(25)	1.396(5)	N(3)–Ni–N(7)	85.79(12)
N(2)–C(6)	1.348(5)	N(5)–Ni–N(6)	80.08(13)
N(2)–C(7)	1.398(5)	N(5)–Ni–N(7)	157.47(13)
N(1)–C(1)	1.341(5)	N(6)–Ni–N(7)	78.37(13)
N(1)–C(5)	1.355(5)		
N(7)–C(30)	1.426(5)		
N(8)–C(31)	1.426(5)		
N(3)–N(4)	1.266(5)		
N(7)–N(8)	1.262(4)		
C(25)–C(30)	1.411(5)		
C(7)–C(8)	1.417(6)		

dyl-N, deprotonated amido-N, and azo-N atoms are *cis*, *trans*, and *cis*, respectively. The chelate bite angles of two L¹¹(-) ligands are closely similar but are considerably less than the ideal octahedral value (90°). As a consequence, the Ni^{II}N₂(pyridyl)N₂(amide)N₂(azo) coordination environment is severely distorted from ideal octahedral geometry. The *cis* angles span a wide range, 78.37(13)–108.80(13)°. The angles between *trans* atoms are in the range, 157.35(14)–171.17(14)°. The Ni–N_{am} (am = amide) bond lengths [1.994(3) and 2.008(3) Å] are the shortest and the Ni–N_{azo} bond lengths [2.189(3) and 2.196(3) Å] are the longest. The two Ni–N_{py} (py = pyridine) bonds are, however, identical [2.087(3) Å]. The Ni–N_{py} bond distances are appreciably longer than that observed for tetradentate ligand system [L⁵(2-); 1.948(2)–1.960(7) Å; four-coordinate complex] [60] and comparable to hexadentate ligand systems [L⁹(2-), L^{9r}(2-), L¹⁰(2-), and L^{10r}(2-); 2.060(2)–2.096(3) Å] [4d,6n] or longer than (~0.1 Å) that encountered with tridentate ligand system [L⁴(2-); 1.994(7) Å] [8c]. The Ni–N_{am} distances observed here are appreciably longer (~0.15 Å) than that encountered with tetradentate ligand system (four-coordinate complex) [1.847(2)–1.854(2) Å] [60]. However, the distances are

slightly shorter [2.021(3)–2.036(3) Å] than that observed with hexadentate ligand systems [4d,6n]. Notably, the observed Ni–N_{am} distances are appreciably shorter than that observed with tridentate ligand [2.127(8) and 2.135(8) Å] [8c]. Extensive electron delocalization along the ligand backbone is implicated.

It is notable that compared to literature reports [22] the observed Ni–N_{azo} bond distances are quite long (~0.28 Å). Average N=N distance in **1** is 1.264(5) Å. This value is identical to that of free N=N distance [1.264(2) Å] [23a] of a closely similar ligand. It is worth mentioning here that in the reported structures of nickel(II) of similar ligands the observed N=N distance is 1.304(2) Å. Thus it is obvious that in **1** the azo groups coordinate very weakly to the nickel(II) center, implying absence of back-bonding through azo functionality.

3.3. Redox properties

Azo groups undergo facile reduction in free as well as metal-coordinated state, owing to the low-lying nature of the azo π^* orbital [11,12,23]. Due to the presence of azo group in HL¹¹, we examined its electrochemical behavior. The cyclic voltammogram (CVgram) of HL¹¹ in CH₂Cl₂ (containing 0.1 M TBAP as supporting electrolyte) at a platinum working electrode is displayed in Fig. S2 (Supporting material). A quasireversible reductive response is observed at $E_{1/2} = -1.18$ V ($\Delta E_p = 100$ mV), assignable to azo-based reduction [11,12,23].

To investigate (i) the extent of stabilization of the nickel(II) state towards oxidation and whether a possibility corresponding to the accessibility of nickel(III) state could be achieved and (ii) the effect of a coordinated metal ion on azo group reduction of L¹¹(–), CV studies on **1** were performed. Complex **1** exhibits an oxidative response and two reductive responses. The oxidative response at $E_{1/2}$ value of 0.96 V versus SCE ($\Delta E_p = 100$ mV) is assigned as metal-centered (Ni^{III}/Ni^{II}) oxidation (Fig. 4). The reductive responses are at $E_{1/2}$ values of –1.13 V ($\Delta E_p = 130$ mV) and –1.48 V ($\Delta E_p = 270$ mV), assignable to nickel(II)-coordinated azo group reductions. Similar observation was encountered before [23].

The following discussion on the $E_{1/2}$ values of Ni^{III}/Ni^{II} redox process for complexes of deprotonated pyridine amide ligands deserves attention. The $E_{1/2}$ values (versus SCE) in CH₂Cl₂ for [Ni^{II}(L¹¹)₂] (**1**) and [Ni^{II}(L⁹)] [6n] complexes are 0.96 and 0.84 V [4d], respectively. The corresponding value for the complex [Et₄N]₂[Ni^{II}(L⁴)₂]·2H₂O in CH₃CN is 0.05 V [8c], which is the lowest. However, the effect of charge on the redox process cannot be ig-

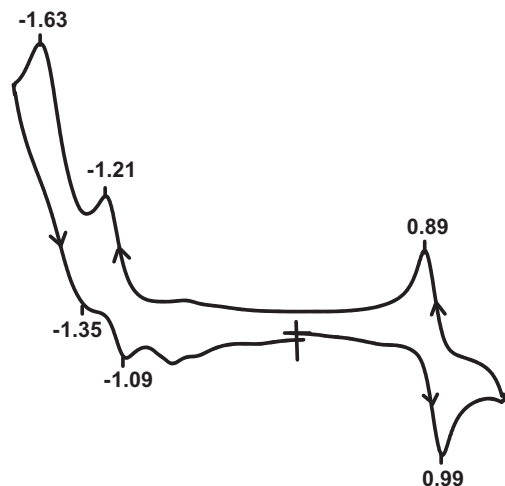


Fig. 4. Cyclic voltammogram (100 mV/s) of ~1 mM solution of [Ni^{II}(L¹¹)₂] (**1**) in CH₂Cl₂ (0.1 M in TBAP) at a platinum working electrode. Indicated potentials (in V) are vs. SCE.

nored. Compared to [Ni^{III}(L⁴)₂][–]/[Ni^{II}(L⁴)₂]^{2–} redox process involving 2– → 1– change in charge during oxidation, the [Ni^{III}(L⁹)⁺]/[Ni^{II}(L⁹)] and [Ni^{III}(L¹¹)₂]⁺/[Ni^{II}(L¹¹)₂] redox processes involve 0 → 1+ change in charge. The lowest $E_{1/2}$ value of [Ni^{II}(L⁴)₂]^{2–} is thus understandable. Within this selected family of complexes the present Ni^{III}/Ni^{II} potential (0.96 V) is on the higher side [4d,8c].

3.4. Coulometric generation of [Ni^{III}(L¹¹)₂]⁺ and the properties of such a species

In order to get information about the stability of 1e[–] oxidized form of [Ni^{II}(L¹¹)₂], we generated blackish red solutions of [Ni^{III}(L¹¹)₂]⁺ (see below) by coulometric oxidation (CH₂Cl₂ containing 0.1 M TBAP; 298 K) of brownish red solutions of [Ni^{II}(L¹¹)₂] at 1.2 V versus SCE. Such solutions display the CV response as that of **1** [Fig. S3 (Supporting material)], attesting the stability of the oxidized species. However, now all the responses are reductive in nature. Spectroelectrochemical experiments (298 K) were carried out to monitor the change in the absorption spectral feature as a result of redox interconversion [Fig. S4 (Supporting material)]. In fact, the intensity of the peak at 480 nm decreases and the spectrum approaches to reveal two broad absorptions at 470 nm ($\epsilon = 11\,700$ M^{–1} cm^{–1}) and at 325 nm ($\epsilon = 30\,700$ M^{–1} cm^{–1}). Absorption spectrum of the final solution (298 K), supposedly containing [Ni^{III}(L¹¹)₂]⁺ species, is displayed in [Fig. S5 (Supporting material)]. The band at 470 nm is assigned as due to ligand-to-metal charge-transfer transition. A similar situation was encountered before [4d,8c].

X-band EPR spectral measurements were performed on coulometrically-generated one-electron oxidized form of **1** to ascertain the locus of oxidation ([Ni^{II}(L)₂] → [Ni^{III}(L)₂]⁺ or [Ni^{II}(L)₂] → [Ni^{II}(L(–)(L))⁺). The spectrum in CH₂Cl₂ (containing 0.1 M TBAP) at 300 K exhibits an isotropic and unresolved signal centered at $g_{iso} = 2.13$ [Fig. S6 (Supporting material)], corresponding to a $S = 1/2$ state. This g_{iso} value is close to that of typical nickel(III) complexes ($g \approx 2.13$ – 2.17) [14,24]. The EPR spectrum of such solutions (CH₂Cl₂, containing 0.1 M TBAP) at 120 K contrasts sharply with that recorded at 298 K. The signal (Fig. 5) is predominantly rhombic ($S = 1/2$), with g values at 2.210, 2.087, and 2.001 ($g_{av} = 2.10$; considering only two resolved signals at $g = 2.210$ and 2.087, $g_{av} = 2.13$). In general, d⁷ low-spin nickel(III) ($S = 1/2$) complexes show anisotropic signals at $g_{\perp} = 2.2$ and $g_{\parallel} = 2.0$ for tetragonally elongated octahedral distortion [14,24]. The pattern of g values [g_x (2.210) $\approx g_y$ (2.087) > g_z (2.001) $\approx g_e$] is indicative of a

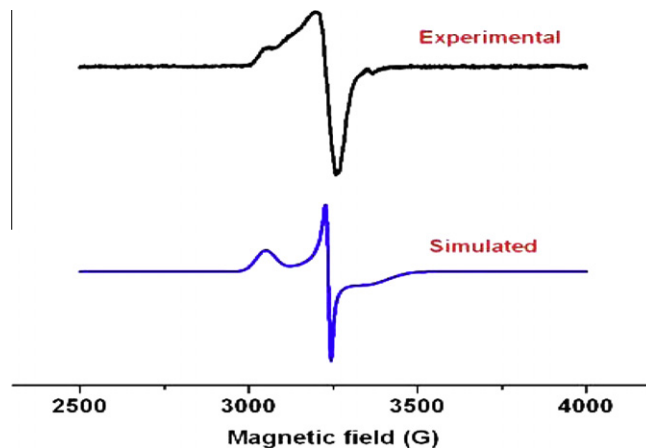


Fig. 5. EPR spectra of coulometrically-generated [Ni^{III}(L¹¹)₂]⁺ species in CH₂Cl₂ (containing 0.1 M TBAP) at 120 K ($\nu = 9.433$ GHz; power = 0.201 mW; receiver gain = 1×10^3 ; modulation frequency = 100 kHz; modulation amplitude = 10 G), and its simulated spectrum. Simulation parameters are described in the text.

dz^2 ground state, where the z-axis is perpendicular to the plane of the molecule. We could reasonably simulate the spectrum observed at 120 K (Fig. 5). The parameters are: $g_{xx} = 2.200$, $g_{yy} = 2.090$, $g_{zz} = 2.001$, $W_x = 56$ G, $W_y = 16$ G, $W_z = 106$ G ($S = 1/2$).

3.5. Computational results

From the crystallographic analysis it is obvious that in the nickel(II) complex $[\text{Ni}^{\text{II}}(\text{L}^{11})_2]$ (**1**) with $\text{Ni}^{\text{II}}\text{N}_2(\text{pyridyl})\text{N}'_2(\text{amide})\text{N}''_2(\text{azo})$ coordination sphere the two pyridyl-N and two deprotonated amido-N efficiently interact with the nickel(II) center, as expected. However, the azo nitrogens do not act as π -acceptors (see above), as anticipated. To extract information about the nature of metal–ligand bonding interactions, spin-unrestricted single-point DFT calculations at the B3LYP level of theory were performed on **1**, $[\text{Ni}^{\text{II}}(\text{L}^4)_2]^{2-}$ [8c], and $[\text{Ni}^{\text{II}}(\text{L}^9)]$ [4d] using their X-ray crystallographic coordinates. An attempt has also been made to rationalize the observed trend in the $\text{Ni}^{\text{III}}/\text{Ni}^{\text{II}}$ redox potential values of **1**, $[\text{Ni}^{\text{II}}(\text{L}^4)_2]^{2-}$, and $[\text{Ni}^{\text{II}}(\text{L}^9)]$. Gross electron population on different

fragments is in Table 3. Quantitative evaluations of the compositions of the highest-occupied molecular orbitals (HOMOs; actually, singly-occupied molecular orbitals SOMOs) and lowest-unoccupied molecular orbitals LUMOs, and the energy of the HOMOs, HOMO–1, LUMO, and LUMO+1 are summarized in Table 4.

Both the α -spin HOMO and LUMO of the nickel(II) complexes are anti-bonding orbitals. The contour surface plots of the HOMO, HOMO–1, LUMO, and LUMO+1 for $[\text{Ni}^{\text{II}}(\text{L}^{11})_2]$ (**1**), $[\text{Ni}^{\text{II}}(\text{L}^4)_2]^{2-}$, and $[\text{Ni}^{\text{II}}(\text{L}^9)]$ are displayed in Fig. 6 and [Fig. S7 (Supporting material)] for **1**, [Fig. S8 (Supporting material)] for $[\text{Ni}^{\text{II}}(\text{L}^4)_2]^{2-}$, and [Fig. S9 (Supporting material)] for $[\text{Ni}^{\text{II}}(\text{L}^9)]$. If the metal–ligand bonding in the complex were purely ionic with no covalent bond contributions, the two HOMOs would be 100% metal-based. The one-electron oxidation will lead to loss of electron from the α -spin HOMO. Because of the anti-bonding nature of the HOMOs, it can be expected that oxidation of the nickel(II) complexes can lead to significant changes in metal–ligand bonding and the redox process will involve both the metal and the ligand. This is corroborated by the electron population analysis of molecular fragments (Table 3).

Table 3

Gross electron population on different fragments of selected nickel(II) pyridine amide complexes from Natural Bond Order (NBO) calculations.

Gross electron population	$[\text{Ni}^{\text{II}}(\text{L}^{11})_2]$ (1)			$[\text{Ni}^{\text{II}}(\text{L}^4)_2]^{2-}$			$[\text{Ni}^{\text{II}}(\text{L}^9)]$		
	Ni s,p	Ni d	Ligand	Ni s,p	Ni d	Ligand	Ni s,p	Ni d	Ligand
α -spin	8.9982	5.0787	157.9231	8.9976	5.0473	165.9551	8.9985	5.1135	126.8880
β -spin	8.9977	3.4327	157.5696	8.9973	3.4237	165.5790	8.9982	3.4878	126.5140
α - β	0.0005	1.6460	0.3535	0.0003	1.6236	0.3761	0.0003	1.6257	0.3740
Total	17.9959	8.5114	315.4900	17.9949	8.4710	331.5341	17.9967	8.6013	253.4020

Table 4

α -Spin frontier molecular orbitals of selected nickel(II) pyridine amide complexes from DFT calculations.

Molecular Orbital	$[\text{Ni}^{\text{II}}(\text{L}^{11})_2]$	$[\text{Ni}^{\text{II}}(\text{L}^4)_2]^{2-}$	$[\text{Ni}^{\text{II}}(\text{L}^9)]$	Orbital contributions from fragments (%)					
	Energy (kcal/mol)	Energy (kcal/mol)	Energy (kcal/mol)	$[\text{Ni}^{\text{II}}(\text{L}^{11})_2]$		$[\text{Ni}^{\text{II}}(\text{L}^4)_2]^{2-}$		$[\text{Ni}^{\text{II}}(\text{L}^9)]$	
				Ni (s,p,d)	Ligand	Ni (s,p,d)	Ligand	Ni (s,p,d)	Ligand
LUMO+1	–48.07	95.63	–30.87	Not calculated					
LUMO	–52.84	95.32	–33.01	0.44	99.56	0.67	99.37	0.56	99.44
HOMO	–117.09	31.94	–118.54	14.74	85.26	20.58	79.42	19.21	80.79
HOMO–1	–120.42	28.36	–122.99	10.51	89.49	20.32	79.68	2.80	97.20

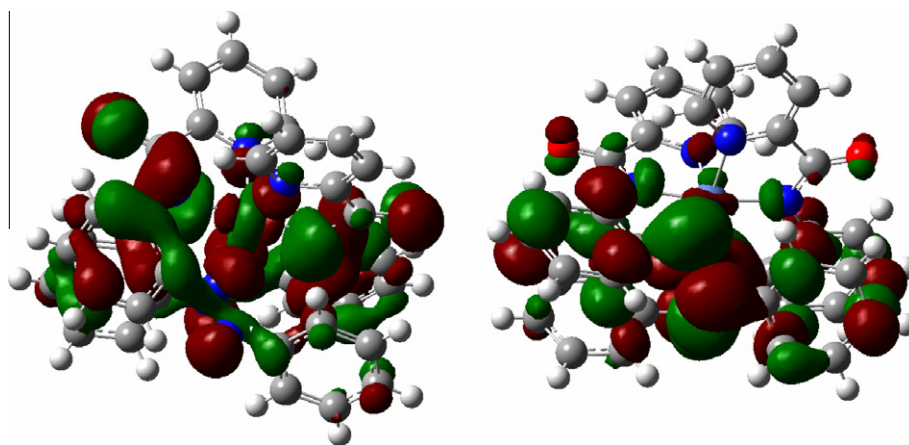


Fig. 6. Contour surfaces of HOMO (left) and LUMO (right) of $[\text{Ni}^{\text{II}}(\text{L}^{11})_2]$ (**1**).

The Mulliken Population Analysis (MPA)-derived electron population of the Ni atoms in **1**, $[\text{Ni}^{\text{II}}(\text{L}^{\text{A}})_2]^{2-}$ and $[\text{Ni}^{\text{II}}(\text{L}^{\text{B}})]$ are 26.51, 26.47, and 26.60 electrons, respectively. For the pure ionic bonding situation the electron population of the Ni atom would be 26 electrons. This electron population results indicate that the chosen complexes are covalently coupled metal–ligand system. Higher metal–ligand covalency reduces the higher atomic charge on the metal ion. Such strong electronic coupling between the metal ion and the deprotonated amide ligands implies that the pyridine amide ligands are redox non-innocent [4e,6b,7,8a,15] and the properties of the corresponding species will strongly depend on the metal–ligand covalency. Consequently, the NPA-derived Ni atomic charges (q_{NPA}) in **1**, $[\text{Ni}^{\text{II}}(\text{L}^{\text{A}})_2]^{2-}$ and $[\text{Ni}^{\text{II}}(\text{L}^{\text{B}})]$ are 1.481, 1.523, and 1.391, respectively. The Natural Population Analysis (NPA)-derived Ni spin-densities (SD_{NPA}) in **1**, $[\text{Ni}^{\text{II}}(\text{L}^{\text{A}})_2]^{2-}$ and $[\text{Ni}^{\text{II}}(\text{L}^{\text{B}})]$ are 1.647, 1.624, and 1.626, respectively.

For **1** the molecular orbital (MO) representations show the HOMO is formed by a combination of metal orbitals (~15%) and ligand orbitals (~85%). The corresponding values for $[\text{Ni}^{\text{II}}(\text{L}^{\text{A}})_2]^{2-}$ are ~20% and ~80% and for $[\text{Ni}^{\text{II}}(\text{L}^{\text{B}})]$ are ~19% and ~81%. For **1** both HOMO and HOMO–1 have Ni d_{z^2} orbital in anti-bonding interaction with ligand orbitals. For $[\text{Ni}^{\text{II}}(\text{L}^{\text{A}})_2]^{2-}$ the HOMO and HOMO–1 have Ni $d_{x^2-y^2}$ and d_{z^2} orbital (anti-bonding interaction with ligand orbitals), respectively. For $[\text{Ni}^{\text{II}}(\text{L}^{\text{B}})]$ the HOMO and HOMO–1 have Ni d_{z^2} and $d_{x^2-y^2}$ (also d_{xy}) (anti-bonding interaction with ligand orbitals), respectively. Specifically, in **1** the ligand contribution in HOMOs is distributed over three components: ~22% (amide), ~6% (pyridyl), and ~14% (azo). For $[\text{Ni}^{\text{II}}(\text{L}^{\text{A}})_2]^{2-}$ the corresponding values are ~39% (amide) and ~6% (pyridyl) and for $[\text{Ni}^{\text{II}}(\text{L}^{\text{B}})]$ the values are ~23% (amide), ~10% (pyridyl), and ~11% (thioether).

For **1** the half-occupied HOMO–1 level is formed by a combination of metal (~11%) and ligand (~89%) orbitals. Thus the HOMO and HOMO–1 levels are to a large extent delocalized over the ligands. For $[\text{Ni}^{\text{II}}(\text{L}^{\text{A}})_2]^{2-}$ and $[\text{Ni}^{\text{II}}(\text{L}^{\text{B}})]$ a similar pattern is observed. However, in these cases the contribution of metal orbitals to HOMO and HOMO–1 levels is higher (about 5%) than that in **1**. The above results point toward a considerable amount of ligand-character, due to strong metal–ligand covalency [25,26], in one-electron oxidized form of these nickel(II) complexes. However, the significant metal character of HOMOs ensures a metal-mediated pathway (partial delocalization of the spin density between a metal orbital and a ligand orbital (with ligand character)). Clearly, electronic communication is mediated by *N*-phenyl-carboxamide/*o*-phenylene moiety on oxidation of nickel(II) center with an appreciable amount of ligand contribution to predominantly metal-centered spin character (cf. EPR spectra) [24].

Given the energies of HOMOs (Table 4) why the $E_{1/2}$ value of $\text{Ni}^{\text{III}}/\text{Ni}^{\text{II}}$ redox process for $[\text{Ni}^{\text{II}}(\text{L}^{\text{A}})_2]^{2-}$ is appreciably cathodic than that of $[\text{Ni}^{\text{II}}(\text{L}^{\text{B}})]$ (**1**) and $[\text{Ni}^{\text{II}}(\text{L}^{\text{C}})]$ is thus understandable. However, given the energies of HOMOs we are not in a position to comment on why the $E_{1/2}$ value of $\text{Ni}^{\text{III}}/\text{Ni}^{\text{II}}$ redox process for **1** is more anodic than that of $[\text{Ni}^{\text{II}}(\text{L}^{\text{C}})]$. Inclusion of solvent effect in the calculation did not alter the trend. Notably, the LUMO and LUMO+1 levels are predominantly ligand in character. The LUMO of **1** has ~51% azo character. The LUMOs of $[\text{Ni}^{\text{II}}(\text{L}^{\text{A}})_2]^{2-}$ and $[\text{Ni}^{\text{II}}(\text{L}^{\text{B}})]$ have ~82% and ~79% pyridyl character. The assignment of observed reductions for **1** as azo-based (see above) is thus justifiable.

4. Summary and conclusions

This work reports the synthesis, structural characterization, and properties of a new six-coordinate nickel(II) complex coordinated by an azo-containing deprotonated pyridine amide ligand providing two pyridyl-N, two amido-N, and two azo-N coordination.

The Ni– N_{am} (am = amide) bond lengths [1.994(3) and 2.008(3) Å] are the shortest and the Ni– N_{azo} bond lengths [2.189(3) and 2.196(3) Å] are the longest. Structural analysis reveals that the 2-pyridinecarboxamido unit effectively interact with the nickel(II) center through pyridine and strongly σ -donating amido nitrogens. Notably, the azo nitrogens remain weakly coordinated to the nickel(II) center. The present investigation provides notable information on the coordination ability of an azo group. As a consequence of being a part of a deprotonated pyridine amide ligand, it does not act as a π -accepting ligand, as one would have expected. The complex displays a facile electron-transfer series [metal-centered and ligand (azo)-centered]. Coulometric generation of one-electron oxidized form of nickel(II) complex has been achieved. We have shown (EPR spectral measurements) that the locus of oxidation in the present nickel(II) complex is best formulated as metal-centered, with delocalization of unpaired electron onto the ligand orbitals. DFT calculations at the B3LYP level of theory of the present complex and two previously reported nickel(II) complexes of solely pyridine amide ligands and along with thioether donor sites have been performed to get information about the nature of metal–ligand bonding in this class of nickel(II) complexes. We are currently probing how subtle changes to pyridine amide ligand electronics, due to incorporation of other donor groups, influence the locus of oxidation in nickel(II) complexes of such ligands of varying denticity.

Acknowledgements

This work is supported by grants from the Department of Science and Technology, Government of India. AKS, SB, and SKB gratefully acknowledge Council of Scientific & Industrial Research (CSIR), New Delhi for research fellowships. RM sincerely thanks DST for J.C. Bose fellowship. We thank Puneet Gupta and Ashish Tiwari for preliminary electron population analysis of molecular fragments.

Appendix A. Supplementary material

CCDC 766087 contains the supplementary crystallographic data for compound **1**. These data can be obtained free of charge from The Cambridge Crystallographic Data Centre via www.ccdc.cam.ac.uk/data_request/cif. Supplementary data associated with this article can be found, in the online version, at [doi:10.1016/j.ica.2010.03.056](https://doi.org/10.1016/j.ica.2010.03.056).

References

- [1] O. Belda, C. Moberg, *Coord. Chem. Rev.* 249 (2005) 727.
- [2] (a) P.K. Mascharak, *Coord. Chem. Rev.* 225 (2002) 201; (b) T.C. Harrop, P.K. Mascharak, *Acc. Chem. Res.* 37 (2004) 253; (c) J.A. Kovacs, *Chem. Rev.* 104 (2004) 825.
- [3] (a) A. Mishra, A. Ali, S. Upreti, R. Gupta, *Inorg. Chem.* 47 (2008) 154; (b) J.-Y. Qi, H.-X. Ma, X.-J. Li, Z.-Y. Zhou, M.C.K. Choi, A.S.C. Chan, Q.-Y. Yang, *Chem. Commun.* (2003) 1294; (c) J.-Y. Qi, L.Q. Qiu, K.H. Lam, C.W. Yip, Z.Y. Zhou, A.S.C. Chan, *Chem. Commun.* (2003) 1058; (d) B.M. Trost, K. Dogra, I. Hachiya, T. Emura, D.L. Hughes, S. Krska, R.A. Reamer, M. Palucki, N. Yasuda, P.J. Reider, *Angew. Chem., Int. Ed.* 41 (2002) 1929; (e) D.A. Conlon, N. Yasuda, *Adv. Synth. Catal.* 343 (2001) 137; (f) T. Hirao, T. Moriuchi, T. Ishikawa, K. Nishimura, S. Mikami, Y. Ohshiro, I. Ikeda, *J. Mol. Catal. A: Chem.* 113 (1996) 117.
- [4] (a) W. Jacob, H. Mishra, S. Pandey, F. Lloret, R. Mukherjee, *New J. Chem.* 33 (2009) 893; (b) A.K. Singh, R. Mukherjee, *Dalton Trans.* (2008) 260; (c) A.K. Singh, R. Mukherjee, *Inorg. Chem.* 44 (2005) 5813; (d) A.K. Singh, R. Mukherjee, *Dalton Trans.* (2005) 2886. and references therein; (e) A.K. Patra, M. Ray, R. Mukherjee, *Inorg. Chem.* 39 (2000) 652; (f) A.K. Patra, M. Ray, R. Mukherjee, *J. Chem. Soc., Dalton Trans.* (1999) 2461; (g) A.K. Patra, R. Mukherjee, *Polyhedron* 18 (1999) 1317. and references therein.

- [5] (a) K. Ghosh, A.A. Eroy-Reveles, M.M. Olmstead, P.K. Mascharak, *Inorg. Chem.* 44 (2005) 8469. and references therein;
(b) A.K. Patra, M.J. Rose, M.M. Olmstead, P.K. Mascharak, *J. Am. Chem. Soc.* 126 (2004) 4780;
(c) D.S. Marlin, M.M. Olmstead, P.K. Mascharak, *Eur. J. Inorg. Chem.* (2002) 859;
(d) J.M. Rowland, M.M. Olmstead, P.K. Mascharak, *Inorg. Chem.* 39 (2000) 5326;
(e) L.A. Tyler, J.C. Noveron, M.M. Olmstead, P.K. Mascharak, *Inorg. Chem.* 39 (2000) 357.
- [6] (a) A. Amiri, M. Amirasr, S. Meghdadi, K. Mereiter, V. Ghodsi, A. Gholami, *Inorg. Chim. Acta* 362 (2009) 3934;
(b) S. Hazra, S. Naskar, D. Mishra, S.I. Gorelsky, H.M. Figgie, W.S. Sheldrick, S.K. Chattopadhyay, *Dalton Trans.* (2007) 4143;
(c) A. Mohamadou, J.-P. Barbier, J. Marrot, *Inorg. Chim. Acta* 360 (2007) 2485;
(d) S. Hubert, A. Mohamadou, C. Gérard, J. Marrot, *Inorg. Chim. Acta* 360 (2007) 1702;
(e) S. Nag, R.J. Butcher, S. Bhattacharya, *Eur. J. Inorg. Chem.* (2007) 1251;
(f) C.F. Fortney, S.J. Geib, F.-T. Lin, R.E. Shepherd, *Inorg. Chim. Acta* 358 (2005) 2921;
(g) J.M. Domínguez-Vera, J. Suárez-Varela, I.B. Maimoun, E. Colacio, *Eur. J. Inorg. Chem.* (2005) 1907;
(h) C.F. Fortney, R.E. Shepherd, *Inorg. Chem. Commun.* 7 (2004) 1065;
(i) A. Das, S.-M. Peng, G.-H. Lee, S. Bhattacharya, *New J. Chem.* 28 (2004) 712;
(j) J.-Y. Qi, Q.-Y. Yang, S.-S. Chan, Z.-Y. Zhou, A.S.C. Chan, *Acta Crystallogr. C* 60 (2004) m210;
(k) C. Jubert, A. Mohamadou, C. Gérard, S. Brandes, A. Tabard, J.-P. Barbier, *J. Chem. Soc., Dalton Trans.* (2002) 2660;
(l) M. Amirasr, K.J. Schenk, S. Meghdadi, *Inorg. Chim. Acta* 338 (2002) 19;
(m) S. Dutta, P.K. Bhattacharya, E. Horn, E.R.T. Tiekink, *Polyhedron* 20 (2001) 1815;
(n) Y. Sunatsuki, T. Matsumoto, Y. Fukushima, M. Mimura, M. Hirohata, N. Matsumoto, F. Kai, *Polyhedron* 17 (1998) 1943;
(o) F.S. Stephens, R.S. Vagg, *Inorg. Chim. Acta* 120 (1986) 165.
- [7] (a) U. Beckmann, E. Bill, T. Weyhermüller, K. Wieghardt, *Inorg. Chem.* 42 (2003) 1045;
(b) S.K. Dutta, U. Beckmann, E. Bill, T. Weyhermüller, K. Wieghardt, *Inorg. Chem.* 39 (2000) 3355.
- [8] (a) A.K. Singh, V. Balamurugan, R. Mukherjee, *Inorg. Chem.* 42 (2003) 6497;
(b) A.K. Patra, M. Ray, R. Mukherjee, *Polyhedron* 19 (2000) 1423;
(c) A.K. Patra, R. Mukherjee, *Inorg. Chem.* 38 (1999) 1388. and references therein;
(d) M. Ray, D. Ghosh, Z. Shirin, R. Mukherjee, *Inorg. Chem.* 36 (1997) 3568. and references therein.
- [9] (a) T.C. Harrop, L.A. Tyler, M.M. Olmstead, P.K. Mascharak, *Eur. J. Inorg. Chem.* (2003) 475;
(b) J.C. Noveron, M.M. Olmstead, P.K. Mascharak, *J. Am. Chem. Soc.* 123 (2001) 3247;
(c) L.A. Tyler, M.M. Olmstead, P.K. Mascharak, *Inorg. Chim. Acta* 321 (2001) 135;
(d) D.S. Marlin, M.M. Olmstead, P.K. Mascharak, *Inorg. Chim. Acta* 297 (2000) 106;
(e) J.C. Noveron, M.M. Olmstead, P.K. Mascharak, *J. Am. Chem. Soc.* 121 (1999) 3553.
- [10] (a) I.V. Korendovych, O.P. Kryatova, W.M. Reiff, E.V. Rybak-Akimova, *Inorg. Chem.* 46 (2007) 4197;
(b) I.V. Korendovych, R.J. Staples, W.M. Reiff, E.V. Rybak-Akimova, *Inorg. Chem.* 43 (2004) 3930;
(c) S.L. Jain, P. Bhattacharyya, H.L. Milton, A.M.Z. Slawin, J.A. Crayston, J.D. Woolins, *Dalton Trans.* (2004) 862;
(d) E. Kolomiets, V. Berl, I. Odriozola, A.-M. Stadler, N. Kyritsakas, J.-M. Lehn, *Chem. Commun.* (2003) 2868;
(e) Z. Shirin, J. Thompson, L. Liable-Sands, G.P.A. Yap, A.L. Rheingold, A.S. Borovik, *J. Chem. Soc., Dalton Trans.* (2002) 1714;
(f) T. Yano, R. Tanaka, T. Nishioka, I. Kinoshita, K. Isobe, L.J. Wright, T.J. Collins, *Chem. Commun.* (2002) 1396.
- [11] W. Kaim, *Coord. Chem. Rev.* 219–221 (2001) 463.
- [12] M. Shivakumar, K. Pramanik, I. Bhattacharyya, A. Chakravorty, *Inorg. Chem.* 39 (2000) 4332. and references therein.
- [13] (a) D.-L. Popescu, A. Chanda, M. Stadler, F.T. de Oliveira, A.D. Ryabov, E. Münck, E.L. Bominaar, T.J. Collins, *Coord. Chem. Rev.* 252 (2008) 2050;
(b) T.J. Collins, R.D. Powell, C. Slebodnick, E.S. Uffelman, *J. Am. Chem. Soc.* 113 (1991) 8419.
- [14] (a) K. Nag, A. Chakravorty, *Coord. Chem. Rev.* 33 (1980) 87;
(b) R.I. Haines, A. McAuley, *Coord. Chem. Rev.* 39 (1981) 77;
(c) S.A. Jacobs, D.W. Margerum, *Inorg. Chem.* 23 (1984) 1195.
- [15] K.P. Butin, E.K. Beloglazkina, N.V. Zyk, *Russ. Chem. Rev.* 74 (2005) 531.
- [16] T. Kaiya, T. Fujiwara, K. Kohda, *Chem. Res. Toxicol.* 13 (2000) 993.
- [17] C.J. O'Connor, *Prog. Inorg. Chem.* 29 (1982) 203.
- [18] R.G. Parr, W. Yang, *Density-Functional Theory of Atoms and Molecules*, Oxford University Press, Oxford, UK, 1989.
- [19] (a) A.D. Becke, *J. Chem. Phys.* 98 (1993) 5648;
(b) C. Lee, W. Yang, R.G. Parr, *Phys. Rev. B* 37 (1998) 785.
- [20] M.J. Frisch, G.W. Trucks, H.B. Schlegel, G.E. Scuseria, M.A. Robb, J.R. Cheeseman, J.A. Montgomery Jr., Vreven, K.N. Kudin, J.C. Burant, J.M. Millam, S.S. Iyengar, J. Tomasi, V. Barone, B. Mennucci, M. Cossi, G. Scalmani, N. Rega, G.A. Petersson, H. Nakatsuji, M. Hada, M. Ehara, K. Toyota, R. Fukuda, J. Hasegawa, M. Ishida, T. Nakajima, Y. Honda, O. Kitao, H. Nakai, M. Klene, X. Li, J.E. Knox, H.P. Hratchian, J.B. Cross, C. Adamo, J. Jaramillo, R. Gomperts, R.E. Stratmann, O. Yazyev, A.J. Austin, R. Cammi, C. Pomelli, J.W. Ochterski, P.Y. Ayala, K. Morokuma, G.A. Voth, P. Salvador, J.J. Dannenberg, V.G. Zakrzewski, S. Dapprich, A.D. Daniels, M.C. Strain, O. Farkas, D.K. Malick, A.D. Rabuck, K. Raghavachari, J.B. Foresman, J.V. Ortiz, Q. Cui, A.G. Baboul, S. Clifford, J. Cioslowski, B.B. Stefanov, G. Liu, A. Liashenko, P. Piskorz, I. Komaromi, R.L. Martin, D.J. Fox, T. Keith, M.A. Al-Laham, C.Y. Peng, A. Nanayakkara, M. Challacombe, P.M.W. Gill, B. Johnson, W. Chen, M.W. Wong, C. Gonzalez, J.A. Pople, Gaussian Inc., Wallingford, CT, 2004.
- [21] Gaussian Inc., Wallingford, CT, 2004.
- [22] L.J. Farrugia, *WINGX Version 1.64*, An Integrated System of Windows Programs for the Solution, Refinement and Analysis of Single-Crystal X-ray Diffraction Data, Department of Chemistry, University of Glasgow, Glasgow, UK, 2003.
- [23] (a) A. Saha, P. Majumdar, S.-M. Peng, S. Goswami, *Eur. J. Inorg. Chem.* (2000) 2631;
(b) P. Banerjee, S.-M. Peng, G.H. Lee, S. Goswami, *Indian J. Chem.* 48A (2009) 25.
- [24] (a) O. Rotthaus, O. Jarjayes, C. Philouze, C.P.D. Valle, F. Thomas, *Dalton Trans.* (2009) 1792;
(b) O. Rotthaus, F. Thomas, O. Jarjayes, C. Philouze, E. Saint-Aman, J.-L. Pierre, *Chem. Eur. J.* 12 (2006) 6953;
(c) O. Rotthaus, O. Jarjayes, F. Thomas, C. Philouze, C.P.D. Valle, E. Saint-Aman, J.-L. Pierre, *Chem. Eur. J.* 12 (2006) 2293;
(d) Y. Shimazaki, S. Huth, S. Karasawa, S. Hirota, Y. Naruta, O. Yamauchi, *Inorg. Chem.* 43 (2004) 7816;
(e) Y. Shimazaki, F. Tani, K. Fukui, Y. Naruta, O. Yamauchi, *J. Am. Chem. Soc.* 125 (2003) 10512.
- [25] K. Ray, T. Petrenko, K. Wieghardt, F. Neese, *Dalton Trans.* (2007) 1552.
- [26] R.K. Szilagy, B.S. Lim, T. Glaser, R.H. Holm, B. Hedman, K.O. Hodgson, E.I. Solomon, *J. Am. Chem. Soc.* 125 (2003) 9158.